Intermittent dynamics and self-organized depinning in propagating fronts

Jørgen Falk, Mogens H. Jensen, and Kim Sneppen
Niels Bohr Institute, Blegdamsvej 17, DK-2100 Copenhagen Ø, Denmark
(Received 14 September 1993)

We study the roughening dynamics of a two-dimensional front where advances are made at minimal pinning sites, while slopes of the front are kept finite by additional lateral growth. The interface self-organizes toward a critical state with long-range correlations in space and time. The dynamics is governed by intermittent bursts which give rise to a scale-invariant avalanche distribution and multiscaling of the temporal roughening. Generalizing a recently proposed theory for the one-dimensional case, we demonstrate that the multiscaling can be explained by the static roughness exponent alone. The correlation between subsequent deposition activities exhibits the same power law as in the one-dimensional case.

PACS number(s): 05.70.Ln, 47.55.Mh, 68.45.Gd, 68.35.Fx

Dynamical roughening interfaces represent a simple class of nonequilibrium extended systems which possess generic scale invariance. A particularly simple example of such systems are interfaces driven locally by uncorrelated Gaussian noise, as discussed by [1]. Interface motion has been experimentally studied in widely different context [2–6] where it generally was found that the height-height correlations of snapshots of the interfaces failed the theoretical predictions systematically [1]. One attempt to remedy this failure was an introduction of power law distributions in the external driving of the interface [7–9]. Another possibility is to investigate under which dynamical conditions long-range correlations spontaneously might appear; that is to investigate when the system becomes self-organized critical [10], a phenomena that can take place in large systems when the overall driving is very slow compared to the microscopic relaxation. One such mechanism was proposed in [11] where a propagating interface in a quenched random medium primarily advanced at the point of minimal global resistance, after which its neighborhood advanced until local slopes remain bounded. An unbounded slope version of this type of interface dynamics, also utilizing the assumptions of invasion percolation [12], has been proposed in [13].

The model of [11] has been extensively studied in one dimension [11,14–17]. In particular it was found that the width W scales with system size L as

$$W^2 = \frac{1}{L}\sum_{i=1}^{L}(h_i - \langle h\rangle)^2 \propto L^{2\chi}, \tag{1}$$

where the static roughness exponent $\chi = 0.63 \pm 0.01$ equals the ratio of perpendicular to parallel correlation length for an interface pinned to the backbone of a directed percolation cluster consistent of connected points of strong pinning. Also it was demonstrated by [16] that the one-dimensional interface exhibits burstlike activity on all scales with a burst size distribution $K(S) \propto S^{-\tau}$, where $\tau = 2/(1+\chi)$ is given by the roughness exponent χ. Finally, the observation of burst dominated activity lead [16, 17] to an explanation of the observed temporal multiscaling [15, 18]

$$A_q(t) = \langle (h_i(t+t') - h_i(t')) - \langle h_i(t+t') - h_i(t')\rangle)^q\rangle^{1/q} \tag{2}$$

$$\approx \langle (h_i(t+t') - h_i(t'))^q\rangle^{1/q} \propto t^{\beta_q} \tag{3}$$

with $\beta_q = (\chi + 1/q)/(\chi+1)$ for $q > 0$ in agreement with the numerical observation of Ref. [15]. Time is measured in units of increased heights per site, and we will see later that the relation for β_q can be easily generalized to higher dimensions. The subtraction of the average displacement in (2) has no significant influence. In fact it appears that without subtraction of the average (3) we obtain a longer temporal scaling regime, because then deviation from scaling only occurs after all sites have changed their height value.

It is now known that the model of Ref. [11] naturally drives the interface into a self-organized critical state, with correlations and dynamics that can be understood from the static scaling exponents of directed percolation [14]. A basic assumption of the model is the separation of time scales that allow us to search for the global minimum of a quenched random noise, before each local adjustment takes place. In the following we investigate how this dynamics wrinkle a two-dimensional front, and we will see that the scaling arguments of [16] can be generalized to explain some of the observed features. The study of higher dimensions is of interest not only for the present model, but in general for dynamical interface models exhibiting burstlike activity [19].

The two dimensional version of [11] is defined on a lattice where each point (x, y, h) is assigned an uncorrelated random number $\eta = \eta(x, y, h)$ in the interval $[0, 1]$. x and y define the horizontal base coordinates, h the height of the interface over the base. At each update we localize the smallest η on the interface. At this place, where the smallest random pinning $\eta(x, y, h)$ is, we add one unit to h and reach a new site with a new random number. If the neighboring gradients of h exceeds 1 we let neighbor sites of the front advance $h(r) \to h(r) + 1$. This process

does not necessarily only involve the nearest four neighbors but should be propagated out in the lattice precisely until all slopes remain less than or equal 1. If we come to the end of the lattice we continue at the other end of it, using periodic boundary conditions. The physical justification for always choosing the minimal pinning site for primary growth can for example be due to an overall instant pressure equilibration. The second main assumption is that of lateral growth that breaks the local rotational symmetry and thereby defines the growth to be fundamentally different from invasion percolation.

The growth dynamics of the model develops first through a transient regime where subsequent updates are uncorrelated but, as time progresses, become correlated on longer and longer distances. After the transient regime one reaches steady state where activities on the front always are highly correlated. It is the scaling properties at this saturated state we consider here.

Figure 1 displays a typical snapshot of the interface after saturation is reached. Although we are in 2+1 dimension we observe a highly rough interface with a roughness exponent $W = \sqrt{\langle (h - \langle h \rangle)^2 \rangle} \propto L^{\chi}$ with $\chi = 0.50 \pm 0.03$ deduced from Fig. 2(a) [20]. For comparison the (2+1)-dimensional Kardar-Parisi-Zhang equation predicts $\chi = 0.40$ [1] whereas the similar Edwards-Wilkinson [21] equation without the nonlinear term only gives logarithmic roughening $W \propto \log(L)$.

When the interface propagate, the chance to advance is largest in the neighborhood of recent propagation [15] because there the typical recent advance has opened for new territory with likely smaller η's. This correlated propagation causes a burstlike activity where subsequent propagation builds up locally and then spreads horizontally. One way to characterize this activity pattern is through the moments: $A_q(\Delta t)$ defined in Eq. 3. Following [16,17] we assume that during time Δt we have a local buildup of a burst given by its extension parallel to the interface $r_{\|}$ and its extension perpendicular to the interface $r_{\perp}$ [22]. Then for each burst

$$r_{\|}^{D}\, r_{\perp} \;=\; \Delta t. \tag{4}$$

The vertical to horizontal buildup is connected by the roughness exponent $\langle r_{\perp} \rangle \;\propto\; \langle r_{\|} \rangle^{\chi}$ where $\langle\,\rangle$ refer to ensemble averaging. The qth moment of the buildup is

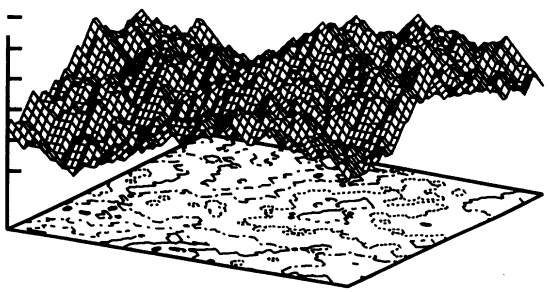

FIG. 1. Static snapshot of a two-dimensional front at saturation. The base plane indicates the structure of the level surfaces of constant value of $h(x, y)$. Note that these appear wrinkled.

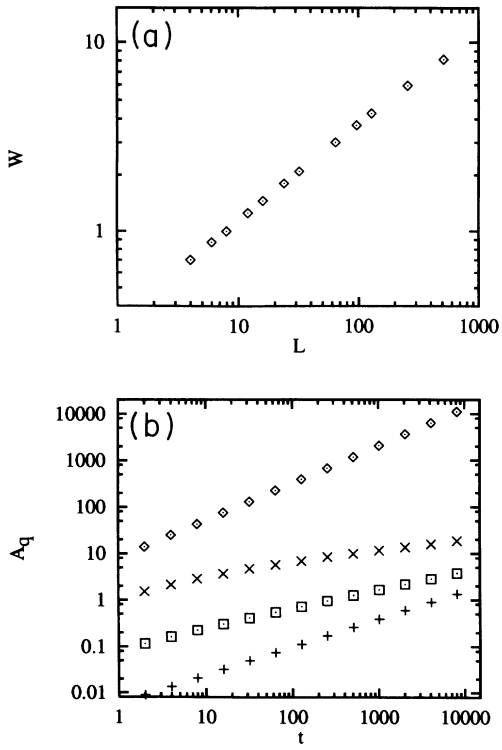

FIG. 2. (a) Width versus system size L. The results are fitted by $W \propto L^{0.50 \pm 0.03}$. (b) Scaling of height-height correlations with time (for system with size L^2, $L = 512$): The diamonds shows the zeroth moment, plusses the second moment, the squares the fourth moment, and crosses the infinite moment.

given by the weighted perpendicular extension

$$\begin{aligned} A_q(\Delta t) \;&\approx\; \langle [h_i(t' + \Delta t) - h_i(t')]^q \rangle^{1/q} \\ &=\; \langle\, r_{\|}^{D}\, r_{\perp}^{q}\, \rangle^{1/q} \;=\; (\Delta t)^{\beta_q}, \end{aligned} \tag{5}$$

with

$$\beta_q \;=\; \frac{q\chi + D}{q\chi + qD} \quad \text{for } q > 0 \quad \text{and} \quad \beta_0 = \frac{D}{\chi + D}. \tag{6}$$

Here we have assumed that for big bursts the ensemble average of products can be replaced by products of ensemble averages. From the numerical simulations shown in Fig. 2(b) we find $\beta_0 = 0.80 \pm 0.01$, $\beta_2 = 0.60 \pm 0.01$, $\beta_4 = 0.40 \pm 0.02$, and $\beta_\infty = 0.20 \pm 0.02$. Thus there is perfect agreement between theory and simulations when we insert $D = 2$. Notice that, in general, for other types of interfaces dynamics dominated by burstlike processes, D does not need to be equal the horizontal dimension. It could be smaller, in that case reflecting either a fractal horizontal growth or a preferred direction of the individual bursts of growth. Notice also that the argument only uses the relation $r_{\perp} \propto r_{\|}^{\chi}$. Here χ is given by the static roughening exponent, but the argument goes beyond this. It could be applied even in case the width of the interface grows beyond all limits and also when $\chi > 1$. The

only requirement is the scaling of vertical to horizontal growth, which then implies the shown interpolation for other moments.

Alternatively to the temporal multiscaling one may characterize the burstlike activity directly through the notion of associated processes [16] which are the avalanches associated to the intermittent advance of the front seen in these types of models. Such quantities have also been used to characterize the dynamics of invasion percolation [23]. To introduce these dynamic quantities we first make the observation that although the noise consists of random numbers equally distributed between 0 and 1 then the noise distribution along snapshots of the interface at saturation is far from random. In fact, as seen in Fig. 3, then the distribution exhibits a steplike function, with nearly no values of η below a certain critical value of $\eta_c = 0.202 \pm 0.002$. However, as is shown with the crosses, the point that is actually chosen as activation centers is always below η_c. These activated values of η may represent the exact time dependent external pressure needed to pass the minimal pinning site, thereby securing the continued marginal propagation of the interface.

Following Ref. [16] we define associated processes as the number of invaded sites between the subsequent breakthrough of a given pinning value η_p selected close below η_c. When η_p is far below η_c, subsequent breakthrough happens often, and we observe exponentially bounded avalanches. Figure 4(a) show that for η_p close below η_c the mass distribution of avalanches approaches a power law (note $S \propto \Delta t$)

$$K(S) = S^{-\tau} f\left(\frac{S}{(\eta_c - \eta_p)^{-\xi}}\right) \tag{7}$$

with exponent $\tau = 1.45 \pm 0.03$. One may also consider the distribution of horizontal extension (area A) of the avalanches

$$K_h(A) = A^{-\tau_A} f_h\left(\frac{A}{(\eta_c - \eta_p)^{-\xi_A}}\right) \tag{8}$$

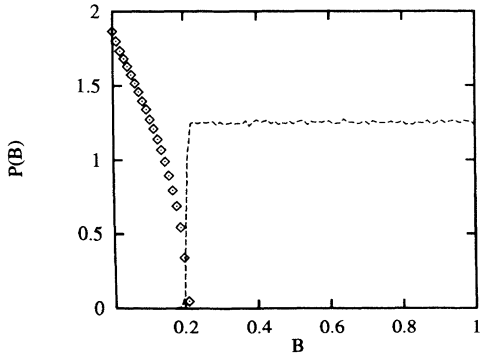

FIG. 3. Ensemble-averaged normalized distribution of quenched noise along saturated members of the propagating two-dimensional front is shown with dashed line. The diamonds show the distribution of quenched noise at points chosen as next activity center, rescaled by a factor 1/4. In contrast to the one-dimensional case, then the probability of selecting a site with value η is close to threshold $\propto (\eta_c - \eta)^{\nu}$ with $\nu = 0.50 \pm 0.05$ different from the linear scaling for the 1D case.

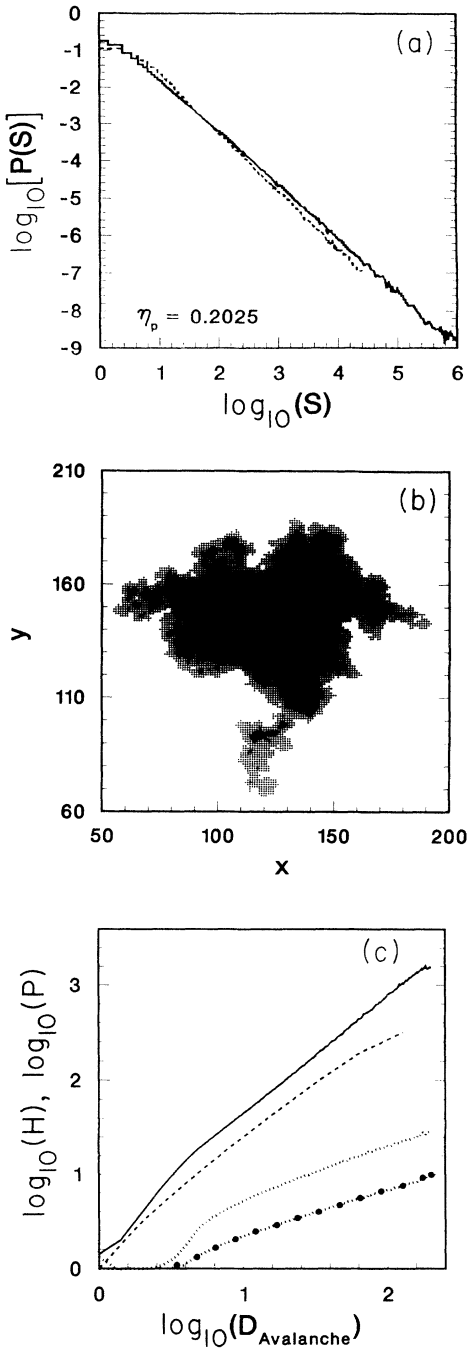

FIG. 4. (a) Distribution of avalanches, corresponding to a punctuation $\eta_p = \eta_c = 0.202$. Solid line displays the total new volume invaded by the avalanche. The dashed line shows the area of the avalanche, measured parallel to the front. (b) Plot of an avalanche, where darkness represents the height. Note the fractal property of the perimeter. (c) Geometrical measures of avalanches. The solid line shows how the number of perimeter sites scales with the "diameter" D of the avalanche, where D is determined as the square root of its area. The dashed line is the number of boxes containing perimeter sites, averaged over many big avalanches, as a function of $256/b$ where b is the length of the box. The dotted lines show, respectively, the scaling of maximal height and of the average height of an avalanche, as function of its "diameter" D.

with exponent $\tau_A = 1.60 \pm 0.05$. One may attempt to understand these scalings by making a one-dimensional cut through the avalanche, assuming both that the avalanche is compact and that the geometry of such a cut is governed completely by the roughness exponent χ. Applying then the procedure of [16] valid for (1+1)-dimensional interface propagation, these assumptions lead to a value of avalanche exponent $\tau = \frac{D+1}{D+\chi} = 1.20$ in disagreement with the numerical results. The reason for this discrepancy, we believe, is due to the fact that the perimeter of an avalanche is fractal [see the visualization in Fig. 4(b)], with dimension $d = 1.20 \pm 0.05$ as seen from the full (or dashed) line in Fig. 4(c). From the avalanche example shown in Fig. 4(b) one may imagine that a particular cut selected on a arbitrary perimeter site will not contain information about the compact center of the avalanche. It is an open problem to understand whether one can associate the fractal dimension of the perimeter and the avalanche exponents τ and τ_A with scaling properties of the front. In this connection we mention that numerically we find that both the average height of an avalanche as well as its maximal height, shown by the dots in Fig. 4(c), scale with the typical avalanche diameter as $D^{0.50 \pm 0.05}$, which is expected because the avalanche is encapsuled by two rough surfaces each characterized by the exponent $\chi = 0.50 \pm 0.03$.

Another feature of the highly correlated propagating front is the distribution of distances X between subsequent events. As shown in Fig. 5(a) the spatial correlation of subsequent depositions scales as

$$C(X, \Delta t) = X^{-\gamma} g\left(\frac{X}{(\Delta t)^{\alpha}}\right), \tag{9}$$

where the numerically observed exponent $\gamma = 2.2 \pm 0.2$ appears identical to the similar exponent measured numerically for the one-dimensional version of the model [24]. In fact this dimensional independence of the activity jump exponent is also observed in the related $h \to -h$ symmetric model of [25], where simulations of dimensions $d = 2 \to 6$ [26] show the same jump exponent (equal to 3.15 ± 0.1) as in the one-dimensional case. We conjecture that also for the model studied here, the exponent γ is dimension independent for $d > 2$, thereby reflecting properties of the involved dynamics that, e.g., goes beyond the dimension dependent roughness exponent χ.

The exponent α takes into account the depletion of activity in a given point when time between activity Δt increases. Notice that $\alpha = \beta_0/D$ where $D = 2$ is the dimension and β_0 denotes the scaling of the horizontal spread of activity shown with diamonds in Fig. 2. Furthermore $\beta_0 = 0.80$ is also the scaling exponent for the decrease in activity in a given point after given activity [$\propto r_\perp/(\Delta t)$ [16]]. In addition one could consider the distribution of waiting times between subsequent advances in a given point (advances are both when a site is actively selected for growth and when it is part of an avalanche), which as seen from the solid line in Fig. 5(b) exhibits a scaling

$$P_{\text{wait}}(t) = t^{-\alpha_{\text{wait}}}, \tag{10}$$

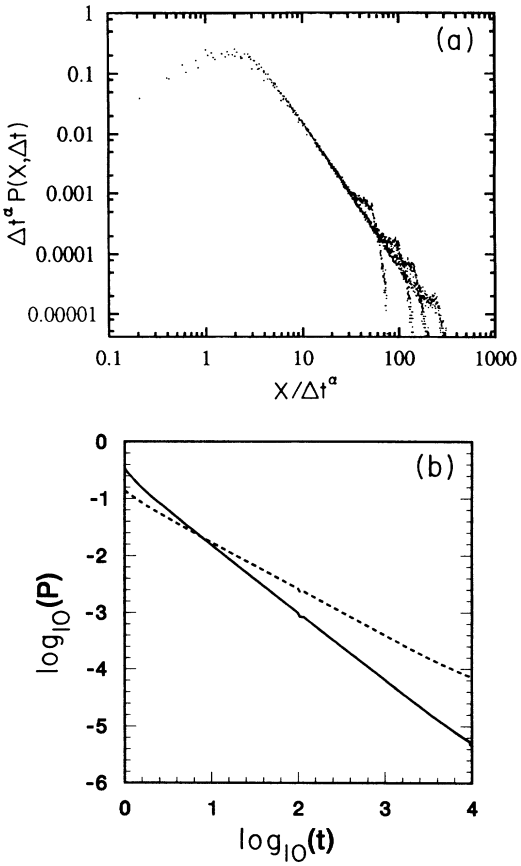

FIG. 5. (a) Spatial distribution of activity centers, separated in time by $\Delta t = 1$, 4, 10, and 50. The simulated system has size L^2 with $L = 256$. We have shown the rescaled distribution, with exponent $\alpha = 0.40$. (b) Solid line shows the numerically measured waiting time distribution between successive updates of the same site is $P_{\text{wait}}(t) = t^{-1.2 \pm 0.1}$. Dashed line shows the hitting frequency after given update, and exhibits a scaling $t^{-\beta_0}$ where $\beta_0 = 0.80 \pm 0.01$ is the exponent for horizontal spread of activity.

with a $\alpha_{\text{wait}} = 1.2 \pm 0.1$ that is smaller than the corresponding one-dimensional waiting time exponent $\alpha_{\text{wait, 1D}} = 1.35 \pm 0.1$ [15]. We lack understanding of both γ and α_{wait}.

In summary we have analyzed the static and dynamic scaling of a two-dimensional propagating front driven at marginal depinning. We observe a burstlike activity giving a temporal multiscaling that is explained by the static roughness exponent χ. Furthermore, the burst activity can be characterized by an avalanche distribution with different exponents for their sizes and horizontal extensions. Contrary to the one-dimensional case, the propagating two-dimensional front exhibits a significant positive value of the skewness $S = \langle (h - \langle h \rangle)^3 \rangle / \langle (h - \langle h \rangle)^2 \rangle^{3/2} = 0.22 \pm 0.03$ when ensemble averaged over random saturated configurations. However, if one does not average over all configurations, but only over configurations where the minimal η value is close to η_c, the value of the skewness drops significantly, to about 0.09 ± 0.02. This, we believe, is because the static scaling proper-

ties of the front at such situations is given by an underlying static structure of connected planes of high η sites. A structure that we believe is symmetric under $h \to -h$, although the used dynamics apparently does not let the front experience all parts of this structure with equal weights (downwards peaks are more easily eliminated than upwards peaks). The scaling property of this structure is in itself not understood and it represents a new class of double directed percolation, that to our knowledge only is mentioned before by [27]. This means that the front propagate with high skewness between the rare situations where all η are above η_c and thus the front is pinned to the underlying static structure. A structure, where instead of percolating along one direction, the directional requirement along two timelike axes, corresponds to having an underlying quenched geometry of connected branching planes, each without overhangs, in three-dimensional time-time-height space.

K. Sneppen thanks the Carlsberg Foundation for financial support. We are grateful to T. Hwa, I. Procaccia, and Y.-C. Zhang for useful comments and discussions.

[1] M. Kardar, G. Parisi, and Y.-C. Zhang, Phys. Rev. Lett. **56**, 889 (1986).
[2] G.B. Springfellow, Rep. Prog. Phys. **45**, 469 (1982); G. Davies, Phys. Bull. **39**, 22 (1988); G.S. Bales, A.C. Redfield, and A. Zangwill, Phys. Rev. Lett. **62**, 776 (1989).
[3] L.M. Galathara, K.S. Kahanda, Xiao-qun Zou, R. Farral, and Po-zen Wong, Phys. Rev. Lett. **68**, 3741 (1992).
[4] M.A. Rubio, C. Edwards, A. Dougherty, and J.P. Gollup, Phys. Rev. Lett. **63**, 1685 (1989); **65**, 1389 (1990).
[5] V.K. Horváth, F. Family, and T.Vicsek, Phys. Rev. Lett. **65**, 1388 (1990), J. Phys. A **24**, L25 (1991).
[6] J. Zhang, Y.-C. Zhang, P. Alstroem, and M.T. Levinsen, Physica A **189**, 383 (1992).
[7] P. Meakin and R. Jullien, Phys. Rev. A **41**, 983 (1990); A. Margolina and H.E. Warriner, J. Stat. Phys. **60**, 809 (1990).
[8] Y.-C. Zhang, J. Phys. **51**, 2129 (1990).
[9] M.H. Jensen and I. Procaccia, J. Phys. (Paris) II **1**, 1139 (1991).
[10] P. Bak, C. Tang, and K. Wiesenfeld, Phys. Rev. Lett. **59**, 381 (1987); C. Tang and P. Bak, *ibid.* **60**, 2347 (1988).
[11] K. Sneppen, Phys. Rev. Lett. **69**, 3539 (1992).
[12] D. Wilkinson and J.F. Willemsen, J. Phys. A **16**, 3365 (1983).
[13] S. Havlin, A.-L. Barabási, S.V.C. Buldyrev, K. Peng, M. Schwartz, H. E. Stanley, and T. Vicsek, in *Proceedings of Granada Conference on "Fractals,"* edited by P. Meakin and L. Sander (Plenum, New York, 1992).
[14] L. H. Tang and H. Leschhorn, Phys. Rev. Lett. **70**, 3833 (1993).
[15] K. Sneppen and M. H. Jensen, Phys. Rev. Lett. **70**, 3833 (1993); *ibid.* **71**, 101 (1993).
[16] Z. Olami, I. Procaccia, and R. Zeitak, Phys. Rev. E. (to be published).
[17] H. Leschhorn and L. H. Tang, Phys. Rev. E. (to be published).
[18] A.-L. Barabasi, J. Phys. A **24**, L1013 (1991); Y.-C. Zhang, J. Phys. (France) I **2**, 2175 (1992).
[19] Z. Olami, I. Procaccia, and R. Zeitak (unpublished).
[20] Y.-C. Zhang (private communication) has shown that $\chi = 1/2$ is the upper limit we could expect in 2D.
[21] S. F. Edwards and D. R. Wilkinson, Proc. R. Soc. London Ser. A **381**, 17 (1982).
[22] In fact, starting the measurement of A_q from an arbitrary time we mostly do not achieve one connected burst. One connected burst only appears when we initiate the measurement exactly when a pinning η close to $\eta_c = 0.205$ is punctuated. By vertical extension of a burst we here only refer to the number of sites activated since initiation. Even when these sites form several disjoint clusters, each of these clusters fulfill individually the scaling between vertical and horizontal extension. The argument of temporal multiscaling applies when one of these clusters always dominates in the thermodynamic limit. This must then be the cluster which during measurement time was started with the punctuation closest to η_c. Thus temporal multiscaling of A_q appears secured by the domination of the recent biggest punctuation event.
[23] L. Furuberg, J. Feder, A. Aharony, and T. Jøssang, Phys. Rev. Lett. **61**, 2117 (1988); S. Roux and E. Guyon, J. Phys. A **22**, 3693 (1989); J.F. Gouyet, Physica A **168**, 581 (1990); N. Martys, M.O. Robbins, and M. Cieplak, Phys. Rev. B **44**, 12 294 (1991).
[24] In 1D the exponent is $2.25 \pm 0.05 = 1 + (\nu + 1)\ \chi$, where $\nu = 1$ is the scaling exponent for the selection of η, as observed by S. Maslov (private communication) through a correction of Ref. [17].
[25] K. Sneppen and M.H. Jensen, Phys. Rev. E **49**, 919 (1994); P. Bak and K. Sneppen, Phys. Rev. Lett. **71**, 4084 (1993); H. Flyvbjerg, K. Sneppen, and P. Bak, Phys. Rev. Lett. **71**, 4087 (1993).
[26] K. Sneppen, P. Bak, and H. Flyvbjerg (unpublished).
[27] A. Barabási, S.V. Buldyrev, S. Havlin, G. Huber, H.E. Stanley, and T. Vicsek, in *Surface disordering, Growth Roughening and Phase Transitions*, edited by R. Jullien, J. Kertesz, P. Meakin, and D.E. Wolf (Nova Science, New York, 1992); see also S. V. Buldyrev, S. Havlin, and H. E. Stanley, Physica A **200**, 200 (1993).

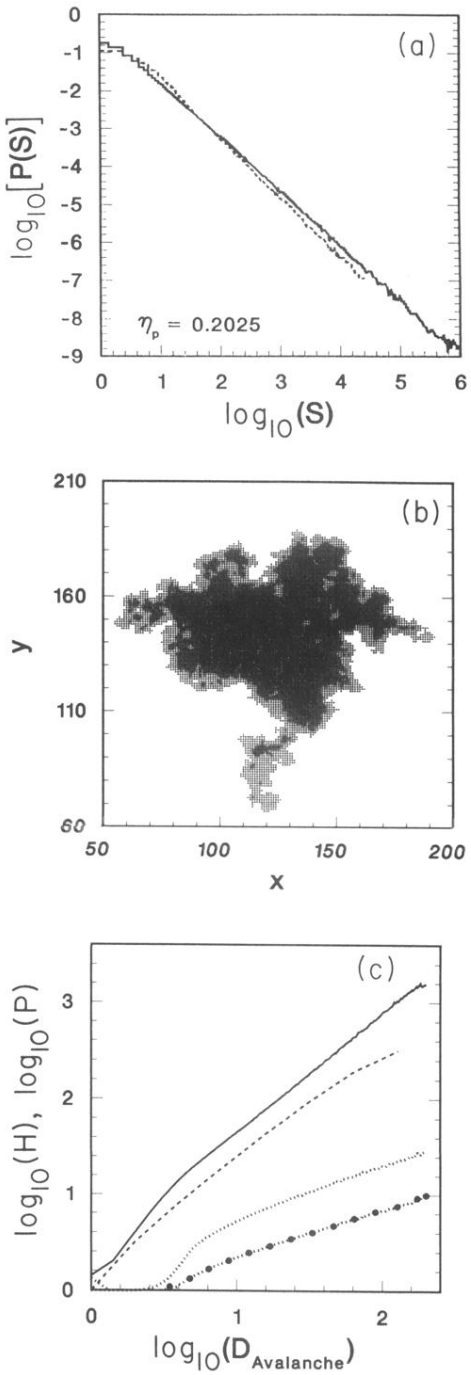

FIG. 4. (a) Distribution of avalanches, corresponding to a punctuation $\eta_p = \eta_c = 0.202$. Solid line displays the total new volume invaded by the avalanche. The dashed line shows the area of the avalanche, measured parallel to the front. (b) Plot of an avalanche, where darkness represents the height. Note the fractal property of the perimeter. (c) Geometrical measures of avalanches. The solid line shows how the number of perimeter sites scales with the "diameter" D of the avalanche, where D is determined as the square root of its area. The dashed line is the number of boxes containing perimeter sites, averaged over many big avalanches, as a function of $256/b$ where b is the length of the box. The dotted lines show, respectively, the scaling of maximal height and of the average height of an avalanche, as function of its "diameter" D.